PITCH-TO-FLY AS A SOARING TACTIC

by Michael L. Steinberger, Central Jersey Soaring Club, New Jersey, U.S.A

Presented at the XXII OSTIV Congress, Uvalde, Texas, USA (1991)

ABSTRACT

This paper introduces a pitch-to-fly theory for efficient cross-country soaring. Analysis, supported by simple measurements, demonstrates that while pitch-to-fly is a direct function of variometer reading and wing loading, it is essentially independent of sailplane L/D. Furthermore, computer simulations demonstrate that even under conditions of rapidly varying lift, pitch-to-fly as a soaring tactic yields cross-country speeds which are within 10% of ideal (and unrealizable) speed-to-fly results. Thus, pitch-to-fly requires only very simple instrumentation, is easy to set up properly in the sailplane, is straightforward to apply in flight, and yields near-optimal cross-country speeds.

Introduction

This paper presents an extension of the classic speed-to-fly theory (see, for example, [1]). The goal of this extension is to make the speed-to-fly theory easier to apply in practice. In particular, it offers improvements in instrumentation, calibration, and flight tactics.

Whereas the speed-to-fly theory is based on the aircraft airspeed and the vertical velocity of the surrounding air, this formulation is based on aircraft pitch attitude and TE-compensated variometer reading. Following the terminology of the speed-to-fly theory, we call the optimum pitch attitude the pitch-to-fly. Pitch attitude is measured by comparing the cockpit deck angle to the horizon, and the TE-compensated variometer is a standard instrument in most sailplanes. Thus, all parameters in this theory are directly measurable using simple instrumentation.

The more surprising result comes in the calibration for pitch-to-fly. Consider that an increase in drag, whether due to aircraft design or bug strike, not only reduces the speed-to-fly, but also reduces the airspeed for a given pitch attitude by increasing the sink rate. The calculations presented here indicate that for a given pitch attitude, this reduction in airspeed is almost identical to the reduction in speed-to-fly. Thus, although it is a direct function of sink rate and wing loading, pitch-to-fly is essentially independent of sailplane L/D. The implication to calibration is that one calculation of pitch-to-fly for a given wing loading can be applied to any aircraft with that wing loading.

The zero point for the pitch scale can be obtained in flight by flying at the minimum sink airspeed, where the angle of attack and sink rate are reasonably well known from fundamental considerations. This makes it possible to bypass the speed-to-fly theory's explicit dependence on the sailplane polar.

Finally, pitch-to-fly implies a straightforward soaring tactic, namely always to adopt the indicated pitch-to-fly. This does not result in exact conformance to speed-to-fly (which is impossible under most conditions); however, time domain simulations indicate that it does result in efficient cross country flight, with the achieved course speed remaining within 10% of ideal speed-to-fly results, even under conditions of rapidly varying lift.

Basic Computations

Figure 1 shows the geometric relationships and basic equations used for this work. the pitch attitude, g, is computed as the difference between the angle of attack, a, and the glide slope angle, ß. In equation 1, the glide slope angle is approximated as the ratio of the sailplane sink rate to the associated airspeed. Note that the sink rate used is that relative to the surrounding air. The effect of air movement is treated in equations 4 and 5.

The angle of attack is calculated from the lift equation for straight and level flight, equation 2. This equation explicitly assumes that the lift coefficient is proportional

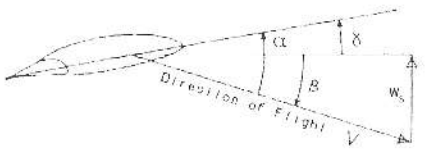

α	Angle of Attack	W	Sailplane Weight
β	Glide Slope Angle	A	Wing Area
δ	Pitch Attitude	ρ	Air Density
V	Sailplane Airspeed	K	Lift vs. AOA Coefficient
W_s	Sailplane Climb Rate	L/D	Sailplane Max Lift/Drag
W_a	Vertical Velocity of Air	V_{LD}	Airspeed for Max L/D
W_{tot}	Variometer Indication	C_i	Coeff. of Induced Drag
		C_p	Coeff. of Parasitic Drag

$$\beta \approx \frac{W_s}{V} \qquad (1)$$

$$W = \frac{1}{2}\rho V^2 A K \alpha \qquad (2)$$

$$\alpha = \frac{2}{\rho V^2 k}\frac{W}{A} \qquad (3)$$

$$W_{tot} = W_s + W_a \qquad (4)$$

$$W_{tot} = V\frac{dW_s}{dV} \qquad (5)$$

FIGURE 1. Basic equations.

to the angle of attack, as is usually the case in cross-country flight. I have estimated the effect of the 2° washout which is typical design practice, and found that its effect on this assumption is negligible. The proportionality constant k is ideally equal to two π for thin airfoils, while some textbooks [2] recommend a rule-of-thumb value of 6.0. This work was done using a k value of 6.08 derived from experimental data [3]. The effect of finite aspect ratio on the value of k was ignored. Through rearrangement of equation 2, equation 3 gives the angle of attack explicitly.

Equations 4 and 5 are a restatement of the classic speed-to-fly theory relating the optimum airspeed to the vertical velocity of the air [1]. The optimum airspeed is that which satisfies equation 5, given equation 4 as a constraint. Note that the variometer reading, w_{tot}', is with respect to the climb rate expected in the next thermal (sometimes called the "speed ring setting"). The speed ring setting was not carried explicitly in the analysis, but was used in the simulations of soaring tactics.

From the equations in Figure 1, the equations in Figure 2 are used to derive a direct relationship between the variometer indication, w_{tot}', and the optimum pitch attitude, g. These equations are based on a model of the sailplane polar which ignores changes in drag coefficient due to changes in Reynolds number or angle of attack. As will be shown in the next two sections, this simplification causes very little loss of accuracy because the optimum pitch angle is insensitive to the exact value of the drag coefficient.

Equation 6 is derived from equation 2, and states the assumption that maximum L/D will occur at a lift coefficient of about .67.

An assumption such as this is necessary to include the angle of attack in the model. The value .67 was chosen as an average over a wide variety of sailplanes. Better results could be obtained by using the lift coefficient appropriate for an individual aircraft. Similarly, it is recommended that one use the lift coefficient for the individual aircraft at minimum sink airspeed when calibrating the pitch attitude in flight.

The sailplane polar assumed is given in equation 7, with the coefficients of induced and parasitic drag given in equations 8 and 9, respectively. Equations 8 and 9 were derived in such a way that they result in the right maximum L/D at the right airspeed. Both coefficients are chosen to be negative so as to keep the sense of the sailplane sink rate, w_s, consistent.

Equations 10 through 12 are used to determine the optimum pitch attitude for a given variometer indication. This is done in a reverse manner by first finding the airspeed at a given pitch attitude, and then finding the variometer reading which would indicate flight at the correct speed-to-fly. Since each of these equations has a unique solution, the relationships can be reversed using a computer search algorithm. Newton's method was used directly for the work reported here. Equations 1, 3, and 7 were combined to derive equation 10. Equation 10 is solved using the quadratic theorem to yield equation 11. Finally, the airspeed given in equation 11 can then be used in equation 12, which is derived from equations 5

$$V_{LD} \approx \sqrt{\frac{3}{\rho}\frac{W}{A}} \qquad (6)$$

$$w_s = \frac{C_i}{V} + C_p V^3 \qquad (7)$$

$$C_i = \frac{-V_{LD}^2}{2L/D} \qquad (8)$$

$$C_p = \frac{-1}{2L/D\,V_{LD}^2} \qquad (9)$$

$$\delta = \frac{C_i}{V^2} + C_p V^2 + \frac{2}{\rho K}\frac{W}{A}\frac{1}{V^2} \qquad (10)$$

$$V^2 = \frac{\delta - \sqrt{\delta^2 - 4C_p\left(\frac{2}{\rho K}\frac{W}{A} + C_i\right)}}{2C_p} \qquad (11)$$

$$w_{tot} = 3C_p V^3 - \frac{C_i}{V} \qquad (12)$$

FIGURE 2. Model equations.

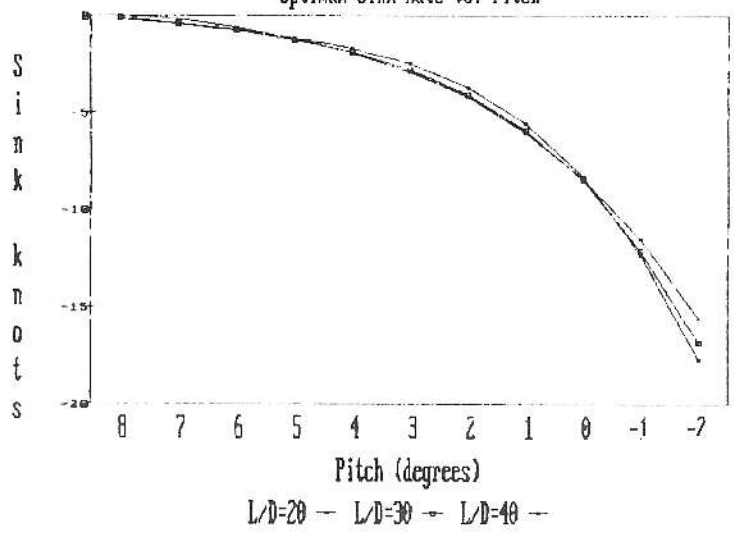

FIGURE 3. Pitch-To-Fly versus L/D for a maximum L/D speed of 50 knots. Variometer reading as a function of optimum pitch attitude is essentially independent of sailplane L/D.

and 7.

Model Results

The above equations predict, as expected, that for the same pitch attitude, a greater L/D will result in a substantially faster airspeed. The surprising result, however, is shown in Figure 3, where the variometer indication for correct speed-to-fly is plotted as a function of pitch attitude for L/D's ranging from 20 to 40, and a V_{LD} of 50 knots. Note that the optimum pitch attitude is almost uniquely a function of variometer reading, and essentially independent of sailplane L/D. It is this insensitivity to sailplane polar which makes pitch-to-fly easy to calibrate for a given aircraft.

While Figure 3 is a numerical result for which I can offer no further direct mathematical justification, perhaps a further clue can be gained by considering the work of Danewid [4], who demonstrated that for a wide range of sailplanes, w_{tot}, is a very simple function of sailplane velocity, minimum, sink speed, and airspeed at a sink rate of two knots.

Comparison with Sailplane Data

The purpose of this section is to compare results implied by the model above with measured results. The first such comparison will be with airspeed vs. pitch attitude data taken on a Blanik L-13. A pitch indicator was made by mounting an inclinometer parallel to the longitudinal axis of the aircraft and mounting a mirror in such a way that the inclinometer could be read in flight. The inclinometer was fitted with a scale with more divisions so that a greater number of precise data points could be taken. Each pitch attitude was held until the airspeed came to equilibrium, and then the airspeed was recorded.

The data measured on the Blanik are shown in Figure 4 along with two calculated curves. The upper curve is that predicted by the general model given in Figure 1. The lower curve was calculated by using the polar data published in the sailplane owner's manual to estimate the glide slope angle, ß. The zero point of the pitch indicator was adjusted to give a good match to the calculated curves at low airspeeds. The conclusions to be drawn from this Figure are that the predictions from the published data follow the measured data quite closely, while the predictions of the general model differ significantly at the higher airspeeds. However, the limitations of the general model notwithstanding, there do not appear to be any fundamental errors in the mathematical analysis presented above.

Figure 5 compares, for an ASW-24, the airspeeds suggested by pitch-to-fly (labeled "From Pitch") with those derived from the published sailplane polar [5] (labeled "From Polar") or a speed-to-fly director (labeled "From Pitch"). To assure that the comparison is made for identical conditions, these speeds are plotted as a function of the vertical velocity of the air, w_a. Note, for reference, that the w_a at V_{LD} should be zero.

For pitch-to-fly, the pitch attitude for each airspeed was calculated using the published data on the sailplane polar at that wing loading. The general model given above was then used to calculate the variometer indication for which the given pitch attitude was optimum. Finally, the sailplane polar data were used to calculate the air vertical velocity given the variometer indication. Thus, this calculation predicts the results obtained by a

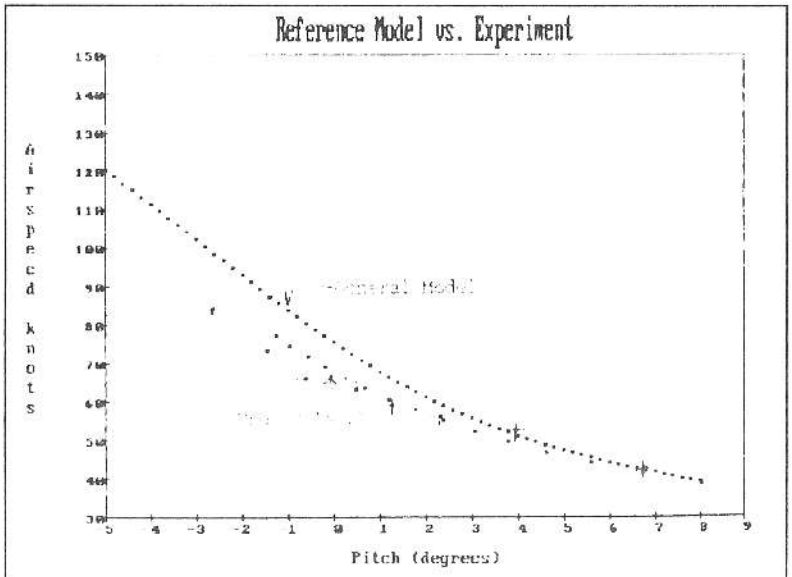

FIGURE 4. Blanik pitch attitude data. Measured airspeed vs. pitch attitude for a Blanik L-13 is compared to that predicted from the general analytic model and that predicted from the published polar.

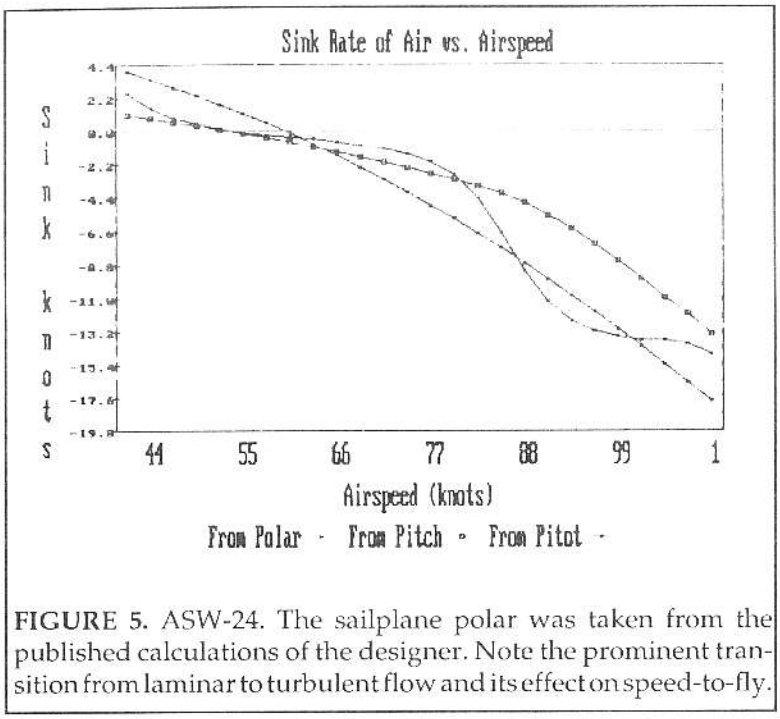

FIGURE 5. ASW-24. The sailplane polar was taken from the published calculations of the designer. Note the prominent transition from laminar to turbulent flow and its effect on speed-to-fly.

pilot who uses the general model to set up the scale on the pitch-to-fly indicator, but then installs and flies it in a real sailplane. The speed-to-fly director was set up using a least-mean square approximation.

With its very noticeable transition from laminar to turbulent flow, the ASW-24 represents an interesting study in the application of the pitch-to-fly theory. The same phenomenon is plainly evident in others of the most modern standard class sailplanes such as the LS-4, LS-7, and Discus. Figure 5 is probably not quite representative of the way the director would be set up in that, instead, it would likely be set up to give accurate results up to 80 knots, with the understanding that the pilot would just "go like heck" if airspeeds greater than 80 knots were required. The pitch-to-fly indicator, on the other hand, gives useful indications in both regimes precisely because pitch-to-fly is insensitive to L/D.

Similar computations were made for the Blanik L-13 using data from the owner's manual and the DG-600 using measured data [6]. For the DG-600, good agreement was obtained between speed-to-fly as computed from measured data and pitch-to-fly according to the general model above. For the Blanik, the airspeed suggested by the general pitch-to-fly model is as much as eight knots faster than that computed from data in the owner's manual. Better agreement might have been attained by assuming a lift coefficient at maximum L/D which was closer to that of the actual aircraft.

Flapped Sailplanes

To be applicable to sailplanes with flaps, the pitch-to-fly theory must be extended to account for flap deflection as well as elevator deflection. Each has a different effect on pitch attitude, and they must therefore be treated separately.

Figure 6 shows the geometric relationships and equations which describe the use of flaps. The equations assume full-span flaps; however, the modification for conventional flaps is straightforward, and yields no additional insight. The effect of flap deflection, x, in equation 13 was derived by Milne-Thompson [7] using the thin airfoil theory.

Equation 14 is an assumption motivated by an analysis of published experimental data. For example, Figure 7 is a re-plot of the experimental data on the UAG 88-143/20 airfoil [8] for a Reynolds number of 1.0×10^6. Rather than plotting lift coefficient separately as a function of angle of attack and drag coefficient, drag coefficient is plotted directly as a function of angle of attack for several flap deflections. In Figure 7, the optimum angle of attack is independent of flap deflection, despite the fact that the range of lift coefficients is much narrower for the +10° flap setting than for the other two settings.

Further evidence is provided by the measured characteristics of the DG-600 sailplane with 17 meter wingtips [6]. For these measurements, the flap setting was adjusted to minimize the profile drag indicated by a drag probe. Using the flap setting chosen, the wing loading, scale drawing as published, and equation 13, I found that the calculated angle of attack remained in a very narrow range over the entire polar.

Given that the elevator will be manipulated in such a way that the angle of attack is constant, the optimum flap deflection can be calculated as a function of variometer indication. An artificial pitch attitude, g, is used in equation 11 in place of g to obtain the optimum variometer reading, and then the same value is used in equation

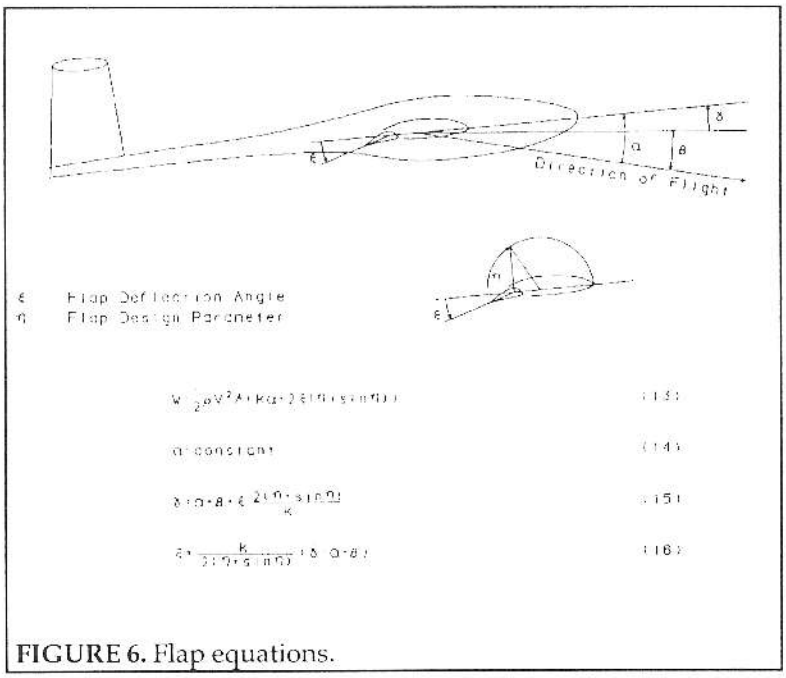

FIGURE 6. Flap equations.

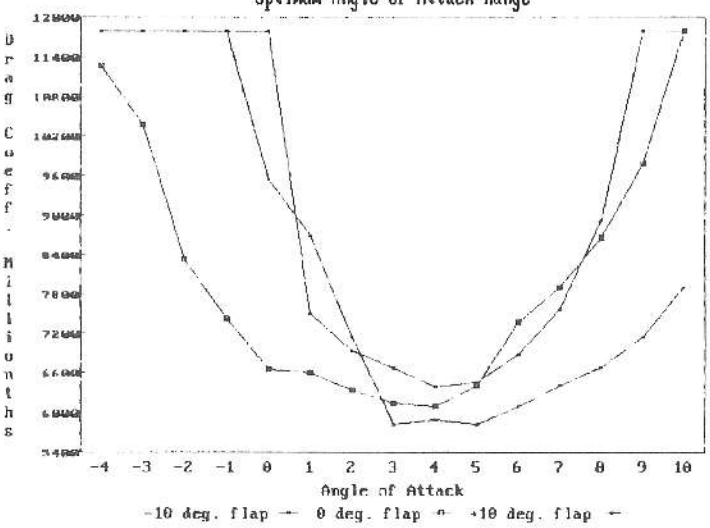

FIGURE 7. Drag coefficient as a function of angle of attack for several flap deflections of the UAG 88-143/20 airfoil. The optimum angle of attack is the same for all flap deflections.

16 to calculate the associated flap deflection.

Soaring Tactics

One of the questions facing especially the inexperienced cross country pilot is exactly how fast to adjust to changing conditions. Making the maneuvers too abrupt will result in excessive drag, while reacting too slowly will result in missed opportunities.

In this section, three soaring tactics are compared using time domain simulations of flight along a flight path with fixed thermal locations. Thermals with a gaussian lift distribution and a one sigma diameter of 70 meters were randomly distributed with an average spacing of 210 meters in an air mass that was assumed to be descending at a rate of 2 knots. Thermal strength was adjusted so that the average air mass movement, including thermals, was zero. This scenario was chosen to simulate as rapidly varying conditions as can be expected in practice.

The three soaring tactics evaluated were: ideal speed-to-fly, pitch-to-fly, and pitch-to-fly with anticipation. The time domain simulations were run with a sample interval of .2 seconds. A speed ring setting of 2 knots was adopted in all cases, and the initial conditions were set to approximately the correct speed-to-fly. At the end of the run, it was assumed that the sailplane would check into a steady 2 knot thermal to bring it back to the initial conditions of altitude and airspeed.

For ideal speed-to-fly, the sailplane was forced to follow the indicated speed-to-fly with no constraints placed on the amount of wing lift necessary to make that happen. It was further assumed that there would be no excess drag due to such maneuvers, and that the only further constraint was conservation of energy. All attempts to make the strict speed-to-fly tactic more realistic were unsuccessful.

For the pitch-to-fly tactic, the pitch attitude of the sailplane was set at each time sample to the optimum predicted by the pitch-to-fly theory for the air vertical velocity encountered. The aerodynamics of the sailplane included the excess induced and profile drag associated with either climbing or diving, although the effects of varying Reynolds number were not included. The sailplane was not allowed to stall, or to generate negative lift. For the pitch-to-fly with anticipation tactic, the pitch attitude was adjusted to the pitch-to-fly for the air 30 meters ahead of the sailplane, about a one second anticipation.

Figure 8 provides a comparison of the airspeeds attained in the speed-to-fly and pitch-to-fly tactics for an ASW-24. As can be seen, there is a substantial difference between the two, with an especially long lag when accelerating to a higher speed. This phenomenon was characteristic of all pitch-to-fly scenarios, and in sharp contrast to the ideal speed-to-fly tactic.

The elapsed times for the cruise and subsequent thermal are given in Table 1 for all three aircraft in the study and all three soaring tactics. For all three of these widely differing aircraft, the attainable flight time using pitch-to-fly comes within 10% of the flight time for ideal speed-to-fly, an effective lower bound for all possible tactics. The results for anticipation mode show that some improvement is possible, and that the optimum tactic has not yet been identified.

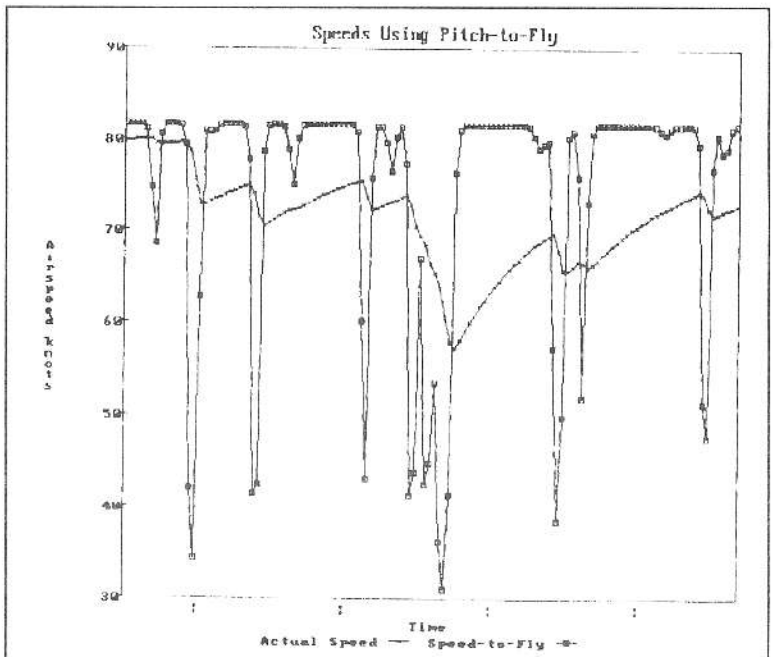

FIGURE 8. Pitch-to-fly airspeed vs. speed-to-fly for ASW-24. The airspeed obtained using pitch-to-fly is contrasted with the ideal speed-to-fly, especially during periods of acceleration.

Tactic	Blanik	ASW-24	DG-600
Ideal Speed-to-Fly	414	264	286
Pitch-to-Fly	432	288	306
Pitch-to-Fly with Anticipation	428	287	303

Table 1: Flight Times (in seconds) for Different Aircraft and Soaring Tactics. The flight time using pitch-to-fly comes within 10% of the ideal speed-to-fly result.

Implementation

All attempts, mechanical or electrical, to put the pilot's head inside the cockpit have so far failed. The only implementation which has proved effective is for the pilot to sight through a translucent scale to the horizon. Depending on the cockpit layout, the scale can either be a plexiglass scale mounted on the instrument panel, or, adhesive-backed vinyl numerals affixed to the canopy. Either way, it must be installed such that the zero point is on the horizon when the sailplane is flown at minimum sink speed.

It turns out that, with the exception of the offset for the zero point, the scale is about the same for all wing loadings. This scale, minus zero point, is shown in Figure 9. The point marked 2 (two knots) usually corresponds closely to the airspeed for maximum L/D. Therefore, the zero point (minimum sink) should be placed below the two knot mark by an amount equal to the difference in pitch attitude between the maximum L/D airspeed and the minimum sink airspeed.

For flapped sailplanes, a copy of the scale is needed for each of the flap positions used in cruising flight (usually three). Each copy is offset from the others by an amount equal to the pitch offset predicted by equation 13 above for the associated flap position. In flight, the pilot uses the scale that goes with the present position of the flaps. An example of a scale for a flapped sailplane is also shown in Figure 9.

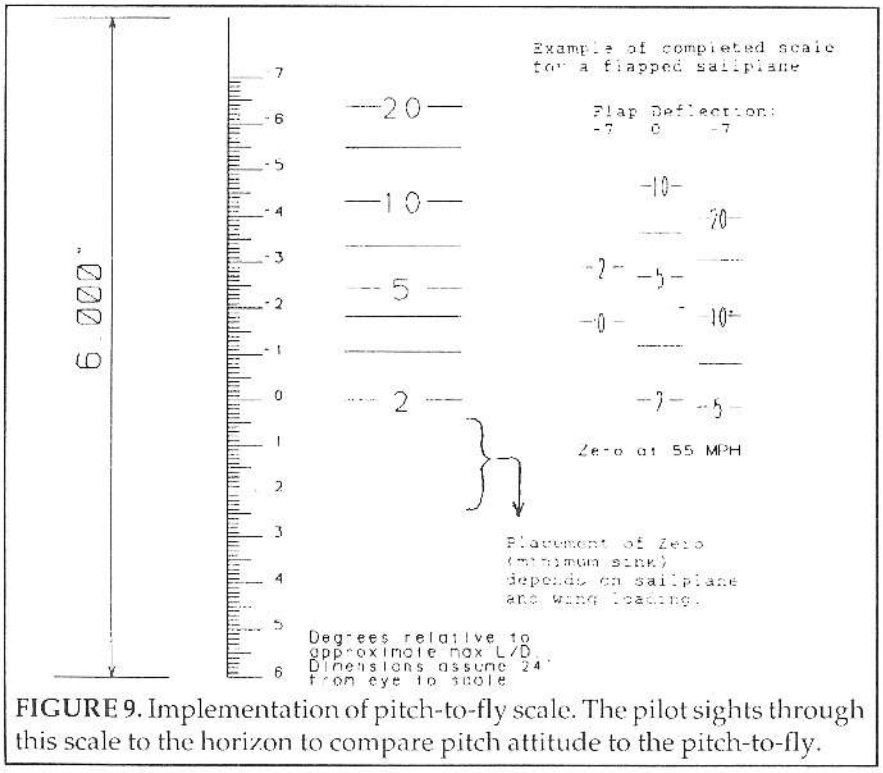

FIGURE 9. Implementation of pitch-to-fly scale. The pilot sights through this scale to the horizon to compare pitch attitude to the pitch-to-fly.

Summary

This paper has introduced a pitch-to-fly theory based on the observation that the optimum pitch attitude is essentially independent of the sailplane L/D. The resulting soaring tactic is straightforward to instrument, calibrate, and apply. Time domain simulations show that this tactic yields results which are within 10% of optimum, even under conditions of rapidly varying lift.

References

1. Reichmann, H., *Cross-Country Soaring*, Thompson Publications, 1978 .
2. Mises, R. von, *Theory of Flight*, Dover Publications, Inc. New York, 1959.
3. Marsden, D. and Toogood, R. W., "Wind Tunnel Tests of a Slotted Flapped Wing Section for Variable Geometry Sailplanes," *Technical Soaring*, Vol. 12, No. 1, pp 4-9, January, 1988.
4. Danewid, R., "A Simple Approximation of the Best-Speed-To-Fly Theory," *Technical Soaring*, Vol. 12, No. 3, pp. 83-7, July, 1988.
5. Boermans, L. M. M. and Waibel, G., "Aerodynamic Design of the Standards Class Sailplane ASW-24," *Technical Soaring*, Vol. 13, No. 3, pp. 72-83, July, 1989.
6. Johnson, Richard H., "A Flight Test Evaluation of the DG-600," *Soaring*, Vol. 53, No. 8, pp. 12-20, August, 1989.
7. Milne-Thomson, L . M., *Theoretical Aerodynamics*, pp . 146-7, Dover Publications, Inc., New York, 1973.
8. Marsden, D. J., "Wind Tunnel Tests of an Ultralight Sailplane Wing Section," *Technical Soaring*, Vol. 14, No. 1, pp. 7-12 January, 1990.